Chemical Engineering

Iranian Journal of Oil & Gas Science and Technology, Vol. 6 (2017), No. 4, pp. 80-96
http://ijogst.put.ac.ir

Mathematical Modeling and Numerical Simulation of CO_2 Removal by Using Hollow Fiber Membrane Contactors

Mohammad Mesbah[1*], Masumeh Jafari[2], Ebrahim Soroush[3], and Shohreh Shahsavari[4]

[1] M.S. Student, Young Researchers and Elites Club, Science and Research Branch, Islamic Azad University, Tehran, Iran
[2] Ph.D. Candidate, Russ College of Engineering and Technology, Ohio University, Athens, OH
[3] M.S. Student, Young Researchers and Elites Club, Ahvaz Branch, Islamic Azad University, Ahvaz, Iran
[4] M.S. Student, Department of Chemical Engineering, Sahand University of Technology, Tabriz, Iran

Received: October 31, 2016; *revised:* December 31, 2016; *accepted:* January 07, 2017

Abstract

In this study, a mathematical model is proposed for CO_2 separation from N_2/CO_2 mixture using a hollow fiber membrane contactor by various absorbents. The contactor assumed as non-wetted membrane; radial and axial diffusions were also considered in the model development. The governing equations of the model are solved via the finite element method (FEM). To ensure the accuracy of the developed model, the simulation results were validated using the reported experimental data for potassium glycinate (PG), monoethanol amine (MEA), and methyldiethanol amine (MDEA). The results of the proposed model indicated that PG absorbent has the highest removal efficiency of CO_2, followed by potassium threonate (PT), MEA, amino-2-methyl-1-propanol (AMP), diethanol amine (DEA), and MDEA in sequence. In addition, the results revealed that the CO_2 removal efficiency was favored by absorbent flow rate and liquid temperature, while the gas flow rate has a reverse effect. The simulation results proved that the hollow fiber membrane contactors have a good potential in the area of CO_2 capture.

Keywords: Gas Separation, CO_2 Capture, Chemical Absorption

1. Introduction

It is well known that the emission of the greenhouse gases such as carbon dioxide (CO_2), which is accounted for about 80% of greenhouse gas emission, is associated with global warming and climate change (Herzog et al., 2000). While there are veracious natural sources of CO_2 emission, the emissions associated with human related activities are the main reason of carbon dioxide increase in the atmosphere in recent decades. The main human related CO_2 emission is the combustion of fossil fuels (oil, natural gas, and coal). However, 80% of the world's total energy sources is supplied by fossil fuels (Wang et al., 2004). On the other hand, concentrated CO_2 is needed for some industrial applications such as enhanced oil recovery (Herzog, 2001). Therefore, the development of CO_2 capture methods is so attractive (Esmaili and Ehsani, 2014, Rahmandoost et al., 2014).

* Corresponding Author:
Email: m_mesbah@alum.sharif.edu

Several CO_2 capture techniques have been developed over the years, including adsorption, chemical and physical absorption, cryogenic distillation, molecular sieve adsorption, and gas-separation membrane. Among these techniques, the absorption of CO_2 into alkanolamine solutions (such as monoethanol amine (MEA), diethanol amine (DEA), triethanol amine (TEA), and methyldiethanol amine (MDEA)) using towers and other traditional contactors is the most widely used method (Lyngfelt and Azar, 1999; Zhao et al., 2008; Oexmann and Kather, 2009; Tuinier et al., 2010). Nevertheless, some problems arise from using conventional absorption methods such as flooding, foaming, channeling, air entrainment, and high energy consuming (Al-Marzouqi et al., 2008; Lin et al., 2008). Membrane contactors are the answer to these problems (Gabelman and Hwang, 1999). The idea of combining absorption by chemical solvent and membrane separation technology was proposed by Qi and Cussler (Qi and Cussler, 1985). Hollow fiber membrane contactors (HFMC) are a group of such contactors, which have been the subject of many studies over the past years (Gabelman and Hwang, 1999; Li et al., 2000; Wang et al., 2004; Li and Chen, 2005; Yan et al., 2007; Lin et al., 2008; Park et al., 2008).

Recently many researchers have been studied CO_2 capture from flue gas. Several factors such as different absorbents, gas and liquid flow rate, and membrane type have been investigated (Lee et al., 2001; Wang et al., 2004; Ren et al., 2006; Atchariyawut et al., 2007; Lu et al., 2007; Yan et al., 2007; Al-Marzouqi et al., 2009; Faiz and Al-Marzouqi, 2009; Rezakazemiet al., 2011). Wang et al. (2004) studied the effect of Amino-2-methyl-1-propanol (AMP), MDEA, and DEA absorbents on CO_2 capture. Their simulations indicated that AMP and DEA have higher removal efficiency than MDEA. Ren et al. (2006) studied CO_2 capture by poly(vinylidene fluoride) (PVDF) hollow fiber membranes. Lu et al. (2007) investigated the effect of AMP and piperazine (PZ) activators on CO_2 removal. Their results showed that the mass-transfer fluxes of activated solutions were much higher than that of the non-activated solution. Yan et al. (2007) used MEA, MDEA, and potassium glycinate (PG) as absorbents for CO_2 capture from flue gas. The experiments were conducted in polypropylene (PP) hollow fiber membrane contactors. They concluded that the PG absorbent is more suitable than MEA and MDEA because it has a lower potential of membrane wetting (which has a direct effect on removal efficiency) and higher reactivity toward CO_2 compared to MEA and MDEA. Kazemi et al. (2011) studied experimentally and theoretically simultaneous removal of CO_2 and H_2S through a HFMC using MDEA as a chemical absorbent. Their results indicated that MDEA is very efficient for H_2S removal.

In this study, CO_2 absorption with different absorbents, namely MEA, MDEA, DEA, AMP, PG, and potassium threonate (PT), is simulated in the case of non-wetted HFMC. The proposed model is validated using experimental data. The effects of different factors, including gas velocity, absorbent temperature, absorbent concentration, and hollow fiber membrane module specification for the preferred absorbent were investigated using the proposed model.

2. The Model development

A comprehensive 2D mathematical model has been developed for the separation of CO_2 from CO_2/N_2 mixture through a hollow fiber membrane contactor including 7000 fibers. Three different kinds of aqueous solutions were studied as an absorbent to compare the capability of the solvent for CO_2 removal. The model was proposed based on "non-wetted mode". The schematic of the hollow fiber membrane used in the present work is shown in Figure 1.

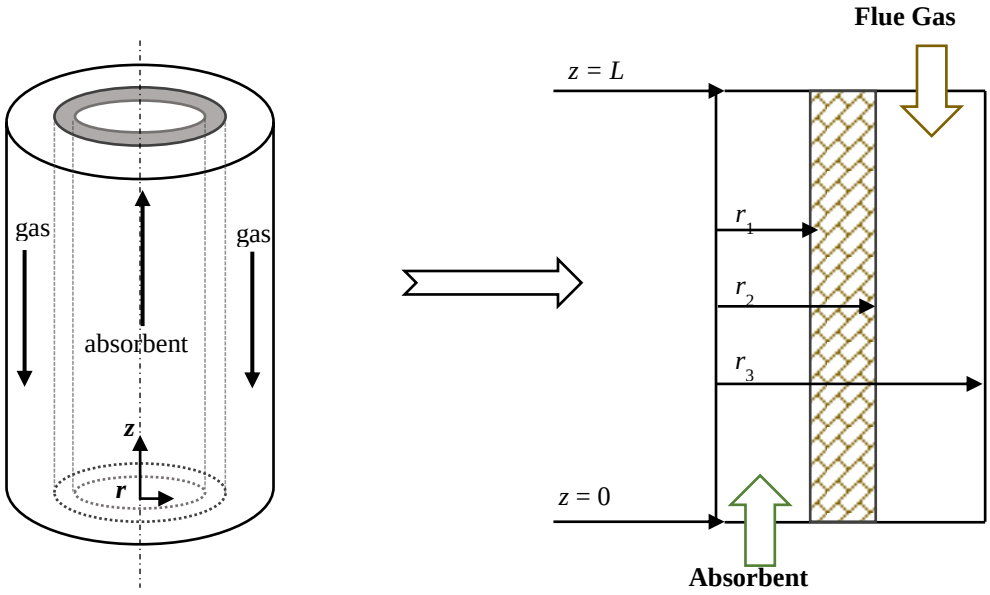

Figure 1
A schematic of hollow fiber membrane contractor.

One of the fibers in the membrane module surrounded by a laminar gas flow has been simulated. The hollow fiber membrane consisted of three sections: (1) tube side, (2) membrane, and (3) shell side. The flue gas, including a mixture of nitrogen and carbon dioxide, is fed downward into the shell side at $z=L$. On the tube side, the fully developed laminar flow solvent is fed upward at z=0. Only the carbon dioxide portion of the gas flow is removed from the gas mixture by diffusing through the membrane and will then be absorbed by the solvent. Figure 2 represents the cross sectional area of the hollow fiber membrane contractor. Based on Happel's free surface model (Happel, 1959), only a portion of fluid enveloping the fiber is considered and could be approximated as a circular cross section.

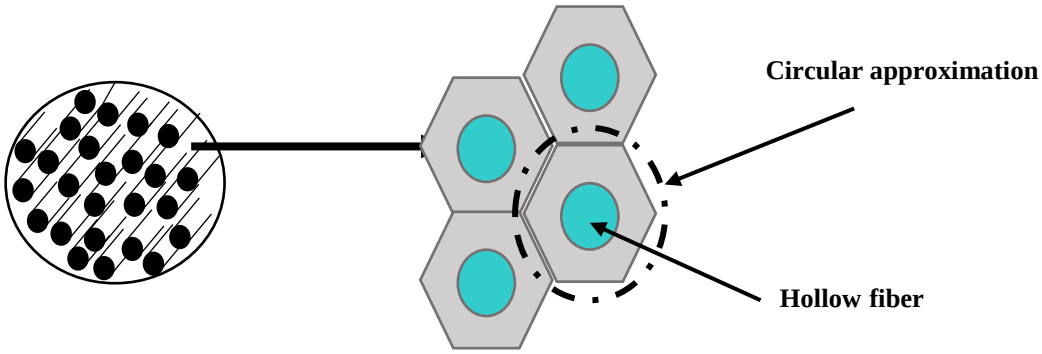

Figure 2
The cross sectional area of the hollow fiber membrane contractor.

The assumptions for the simulation can be summarized as given below.

1. The simulation conditions is steady-state and isothermal;
2. Velocity profiles for the fluid through hollow fiber are fully developed;
3. The gas mixture is considered as an ideal gas;
4. A non-wetted mode in which the gas mixture fills the membrane pores is assumed;

5. Henry's law is applied to gas-liquid interface;
6. No homogenous reaction takes place at the shell side.

2.1. Mass transfer equations

a) Tube side

The steady state continuity equation for the transport of CO_2 in the tube side, consisting of Fick's law to predict the diffusion flux, can be written by.

$$D_{i-tube}\left[\frac{\partial^2 C_{i-tube}}{\partial r^2}+\frac{1}{r}\frac{\partial C_{i-tube}}{\partial r}+\frac{\partial^2 C_{i-tube}}{\partial z^2}\right]=V_{z-tube}\frac{\partial C_{i-tube}}{\partial z}-R_i \tag{1}$$

where, i refers to CO_2 or absorbent, and *Ri* is the reaction rate of component i. It is assumed that the velocity distribution in the tube side follows the Newtonian laminar flow (Bird et al., 1960):

$$V_{z-tube}=2(\overline{V}_{tube})\left[1-\left(\frac{r}{R_1}\right)^2\right] \tag{2}$$

The boundary conditions on the tube side are considered as:

at z= 0, $C_{CO_2-tube}=0$ and $C_{adsorbent-tube}=C_{initial}$ (3)

i stands for the solvents, namely MEA, DEA, AMP, MDEA, PG, and PT.

at $r=R_1$, $C_{i-tube}=C_{i-membrane}\times m$ (4)

at $r=0$, $\frac{\partial C_{i-tube}}{\partial r}=0$ (symmetry) (5)

where, *m* is the partition coefficient of CO_2 in the solvent.

b) Membrane

As the membrane is assumed to be non-wetting and only CO_2 could diffuse through it, the steady state continuity equation for the transport of CO_2 in the membrane can be written as follows:

$$D_{CO_2-membrane}\left[\frac{\partial^2 C_{CO_2-membrane}}{\partial r^2}+\frac{1}{r}\frac{\partial C_{CO_2-membrane}}{\partial r}+\frac{\partial^2 C_{CO_2-membrane}}{\partial z^2}\right]=0 \tag{6}$$

The effective diffusion coefficient of the porous membrane is calculated by Equation 7 (Faiz and Al-Marzouqi, 2009), where ε and τ are porosity and tortuosity respectively; they are defined by membrane manufacturers.

$$D_{membrane}=D_{solvent\ phase}\left(\frac{\varepsilon}{\tau}\right) \tag{7}$$

The boundary conditions on the shell side are considered as follows:

$$\text{at } r = R_1, \quad C_{CO_2-membrane} = \frac{C_{CO_2-tube}}{m} \tag{8}$$

$$\text{at } r = R_2, \; C_{CO_2-membrane} = C_{CO_2-shell} \tag{9}$$

c) Shell side

The steady state continuity equation for the transport of CO_2 in the shell side can be expressed as given below:

$$D_{CO_2-shell}\left[\frac{\partial^2 C_{CO_2-shell}}{\partial r^2} + \frac{1}{r}\frac{\partial C_{CO_2-shell}}{\partial r} + \frac{\partial^2 C_{CO_2-shell}}{\partial z^2}\right] = V_{CO_2-shell}\frac{\partial C_{CO_2-shell}}{\partial z} \tag{10}$$

The velocity distribution in the shell can be evaluated by considering Happel's free surface model:

$$V_{z-shell} = 2(V)\left[1-\left(\frac{R_2}{R_3}\right)\right]\times\left[\frac{(r/R_3)^2 - (R_2/R_3)^2 + 2\ln(R_2/r)}{3+(R_2/R_3)^4 - 4(R_2/R_3)^2 + 4\ln(R_2/R_3)}\right] \tag{11}$$

Also, Happel's free surface model can be applied to estimating the radius of the shell:

$$R_3 = R_2\sqrt{\frac{1}{(1-\phi)}} \tag{12}$$

where, ϕ is the volume fraction of the void and can be defined as follows:

$$1-\phi = \frac{nR_2^2}{R^2} \tag{13}$$

In which, n is the number of fibers, and R is the module inner radius.

The boundary conditions on the shell side may be defined by:

$$\text{at } z = L, \; C_{CO_2-shell} = C_{CO_2-initial} \tag{14}$$

$$\text{at } r = R_2, \; C_{CO_2-membrane} = C_{CO_2-shell} \tag{15}$$

$$\text{at } r = R_3, \; \frac{\partial C_{CO_2-shell}}{\partial r} = 0 \text{ (insulation)} \tag{16}$$

The reaction rates and transport properties for different absorbents are given in Table 1.

Table 1
Reaction rates and transport properties used in this study (T_g= 298 K, T_l= 298 K, $C_{Absorbent}$= 1 M).

Absorbent	Parameter	Value	Unit	Reference
MEA (1 M)	$D_{CO2\text{-}Tube}$	1.51×10^{-09}	m^2/s	(Versteeg and Van Swaalj, 1988)
	$D_{Absorbent\text{-}Tube}$	9.32×10^{-10}	m^2/s	(Versteeg and Van Swaalj, 1988)
	m	0.8	-	(Versteeg and Van Swaalj, 1988)
	CO_2 Rate of Reaction	$-R_{CO_2}=\frac{C_{CO_2}C_{MEA}}{\frac{1}{6.358}+\frac{1}{\left(9.58\times10^{-6}C_{H_2O}\right)+\left(1.58\times10^{-3}C_{MEA}\right)}}$	mol/(m^3.s)	(Liao and Li, 2002)
DEA (1 M)	$D_{CO2\text{-}Tube}$	1.47×10^{-09}	m^2/s	(Versteeg and Van Swaalj, 1988)
	$D_{Absorbent\text{-}Tube}$	6.32×10^{-10}	m^2/s	(Versteeg and Van Swaalj, 1988)
	m	0.79	-	(Versteeg and Van Swaalj, 1988)
	CO_2 Rate of Reaction	$-R_{CO_2}=\frac{C_{CO_2}C_{DEA}}{\frac{1}{2.375}+\frac{1}{\left(2.20\times10^{-6}C_{H_2O}\right)+\left(4.37\times10^{-4}C_{DEA}\right)}}$	mol/(m^3.s)	(Xu et al., 1996)
AMP (1M)	$D_{CO2\text{-}Tube}$	1.18×10^{-09}	m^2/s	(Saha et al., 1993)
	$D_{Absorbent\text{-}Tube}$	5.67×10^{-10}	m^2/s	(Paul et al., 2007)
	m	0.8	-	(Paul et al., 2007)
	CO_2 Rate of Reaction	$-R_{CO_2}=\frac{C_{CO_2}C_{AMP}}{\frac{1}{0.81}+\frac{1}{\left(2.64\times10^{-6}C_{H_2O}\right)+\left(2.335\times10^{-3}C_{AMP}\right)}}$	mol/(m^3.s)	(Xu et al., 1996)
MDEA (1M)	$D_{CO2\text{-}Tube}$	1.18×10^{-09}	m^2/s	(Versteeg and Van Swaalj, 1988)
	$D_{Absorbent\text{-}Tube}$	6.21×10^{-10}	m^2/s	(Versteeg and Van Swaalj, 1988)
	m	0.82	-	(Versteeg and Van Swaalj, 1988)
	CO_2 Rate of Reaction	$-R_{CO_2}=5.21\times10^{-3}C_{CO_2}C_{MDEA}$	mol/(m^3.s)	(Littel et al., 1992)
PG (1M)	$D_{CO2\text{-}Tube}$	1.42×10^{-09}	m^2/s	(Portugal et al., 2007)

Absorbent	Parameter	Value	Unit	Reference
PT (1M)	$D_{\text{Absorbent-Tube}}$	1.19×10^{-09}	m^2/s	(Hamborg et al., 2008)
	m	1.50	-	(Portugal et al., 2007)
	CO_2 Rate of Reaction	$-R_{CO_2} = 2.42\times10^{16}\exp\left(\frac{-8544}{298}\right)\exp(0.44C_{PG})C_{PG}C_{CO_2}$	$mol/(m^3.s)$	(Portugal et al., 2007)
	$D_{\text{CO2-Tube}}$	1.38×10^{-09}	m^2/s	(Portugal et al., 2008)
	$D_{\text{Absorbent-Tube}}$	8.45×10^{-10}	m^2/s	(Portugal et al., 2008)
	m	1.50	-	(Portugal et al., 2008)
	CO_2 Rate of Reaction	$-R_{CO_2} = 4.13\times10^{8}\exp\left(\frac{-3580}{298}\right)\exp(0.90C_{PT})C_{PT}C_{CO_2}$	$mol/(m^3.s)$	(Portugalet al., 2008)

2.2. Numerical simulation

The governing equations for CO_2 removal related to tube, membrane, and shell are solved numerically using COMSOL Multiphysics software, which uses the finite element method (FEM) for the numerical solution of the governing equations of the model. FEM analysis along with an error control and an adaptive meshing technique is applied using the solver of parallel direct linear solver (PARDISO). This solver is well suited for solving stiff and non-stiff nonlinear boundary value problems. In order to assure the mesh independence of the model, the CO_2 removal efficiency of MEA absorbent (at Vl= 0.0503 m/s; Vg= 0.317 m/s; Tl= 308 K; Tg= 298 K; Volume fraction of CO_2 in gas= 14 vol.%; MEA concentration= 1 M) was investigated at different mesh numbers. The result is shown in Figure 3. As it could be seen from this figure, the efficiency does not change for the number of elements more than 25000, so this value is chosen as the mesh number in this study. The characteristics of HFMC used in numerical simulation are summarized in Table 2.

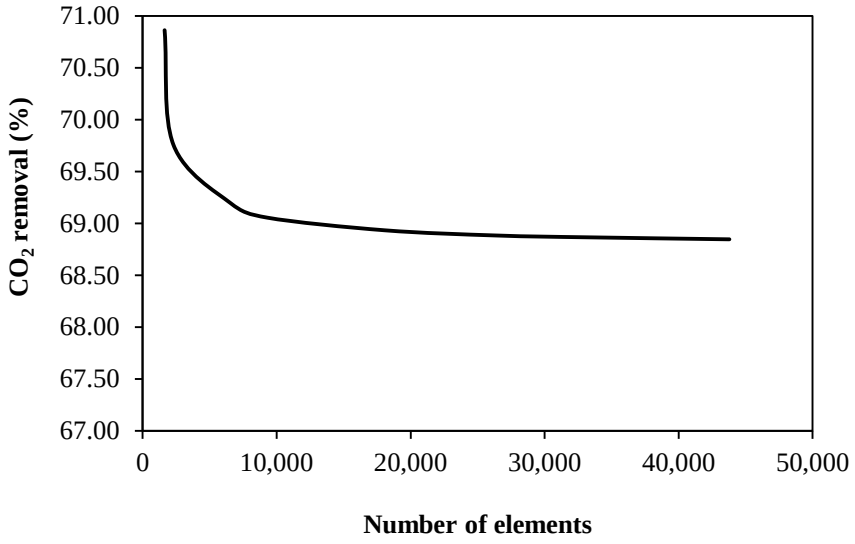

Figure 3
Checking mesh independence (Vl= 0.0503 m/s; Vg= 0.317 m/s; Tl= 308 K; Tg= 298 K; Volume fraction of CO_2 in gas= 14 vol.%; MEA concentration= 1 M).

Table 2
Characteristics of hollow fiber module (Yan et al., 2007).

Parameter	Unit	Symbol	Value
Module inner radius	cm	R	4
Inner radius of fiber	μm	R_1	172
Outer radius of fiber	μm	R_2	221
Length	cm	L	80
Porosity (%)	-	ε	45
Tortuosity	-	τ	1/ ε ¥
The average size of pore	μm	d	0.02×2
Number of fiber	-	n	7000

¥ Estimated from Wakao–Smith equation, τ= 1/ ε (Zhang et al., 2014)

3. Results and discussion

3.1. Model validation

The model was validated using the experimental results from Yan et al. work (Zhang et al., 2014) for CO_2 absorption in MEA, MDEA, and PG. In this section, the results of the model are compared with the experimental data. The removal efficiency of CO_2 may be defined as below:

$$\eta = \frac{(Q_{in} \times C_{in}) - (Q_{out} \times C_{out})}{(Q_{in} \times C_{in})} \tag{17}$$

where, η is removal efficiency of CO_2, and Q_{in} and Q_{out} are the gas flow rates at the inlet and outlet respectively; C_{in} and C_{out} are the concentration of CO_2 at inlet and outlet respectively. The concentration of CO_2 at shell side outlet is obtained using Equation 18.

$$C_{out} = \frac{\iint_{Z=0} C(r)\, dA}{\iint_{Z=0} dA} \tag{18}$$

The CO_2 removal efficiency at different gas velocities for MEA and PG is presented in Figure 4. The effects of CO_2 volume fraction in gas phase on CO_2 removal efficiency of MEA, MDEA, and PG are presented in Figure 5. As it can be seen, the simulation results are in good agreement with the experimental data. The characteristics of the hollow fiber membrane module are given in Table 2.

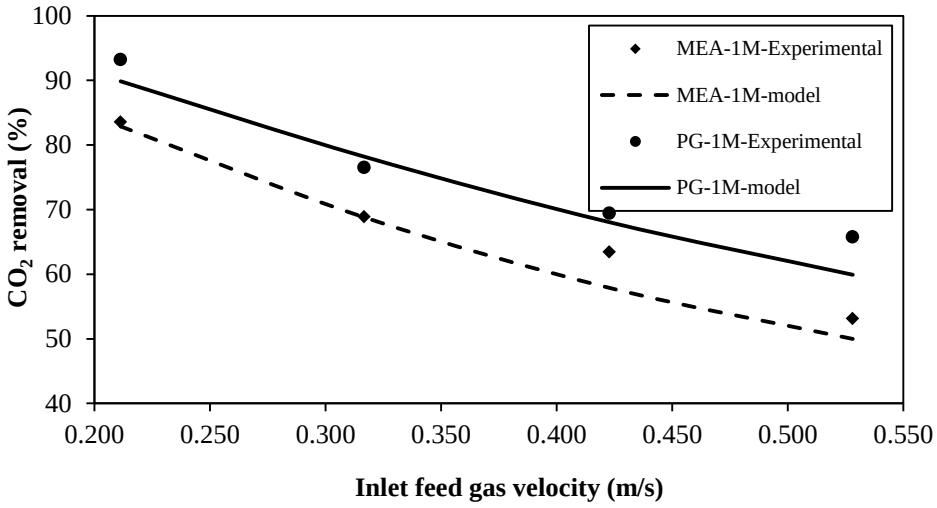

Figure 4
Comparison of the experimental results with the model results for the effect of gas velocity on the CO_2 removal efficiency; Vl= 0.0503 m/s; Tl= 308 K; Tg= 298 K; Volume fraction of CO_2 in gas= 14 vol.%; Absorbent concentration= 1M.

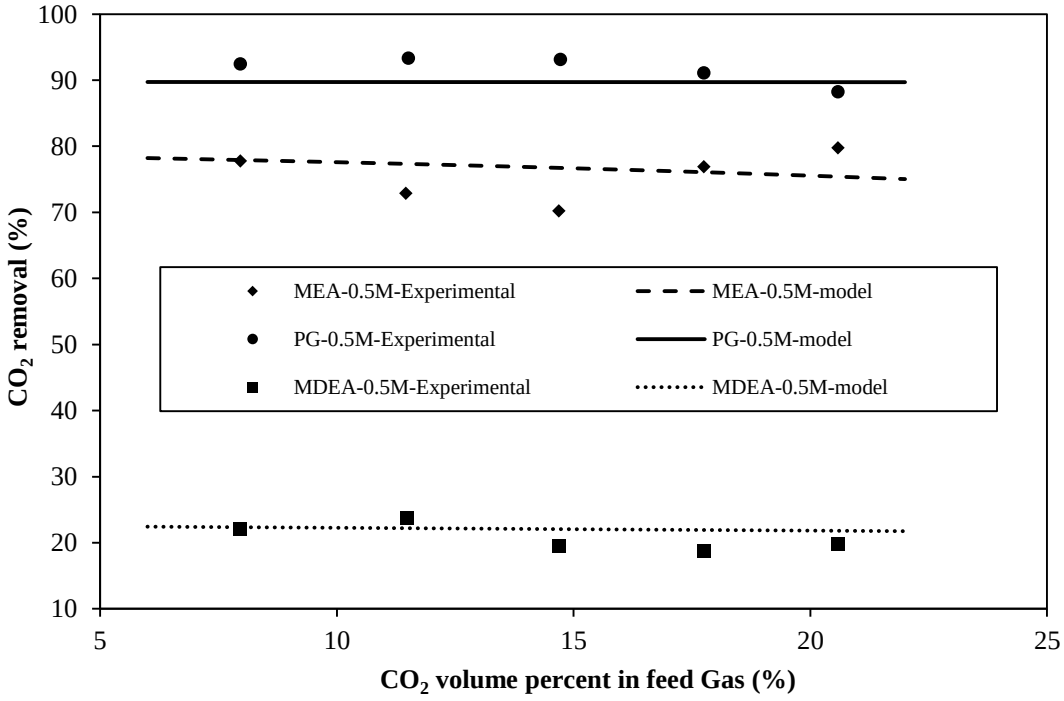

Figure 5
Comparison of the experimental results with the model results for effect of CO_2 in the gas phase on the CO_2 removal efficiency; Vl= 0.0503 m/s; Tl= 308 K; Vg= 0.211 m/s; Tg= 298 K; Absorbent concentration= 0.5 M.

3.2. CO_2 Concentration distribution

Figure 6 indicates the dimensionless concentration distribution of CO_2 when PG is used as the absorbent. The gas mixture containing N_2 and CO_2 enters at the shell side from the top (z=L), where

the concentration of CO_2 is maximized. The fresh chemical absorbent (PG) enters at the tube side from the bottom (z=0), where the concentration of CO_2 is zero. As the gas flows through the shell side, CO_2 transfer across the membrane because the concentration difference (or chemical potential difference) between the shell side and the tube side gradually decreases. It should be noted that the concentration difference is the driving force for the diffusion of CO_2 through the membrane from the shell side to the tube side. CO_2 is transferred to the shell side of the contactor by two mechanisms, diffusion in the radial direction due to the concentration difference and convection in the axial direction. The removal of CO_2 increases by increasing the diffusion of CO_2 through the membrane; therefore, the diffusion mechanism is favorable. Due to non-wetted mode assumption, the concentration of CO_2 at the same z-coordinate in the membrane and the shell side is uniform.

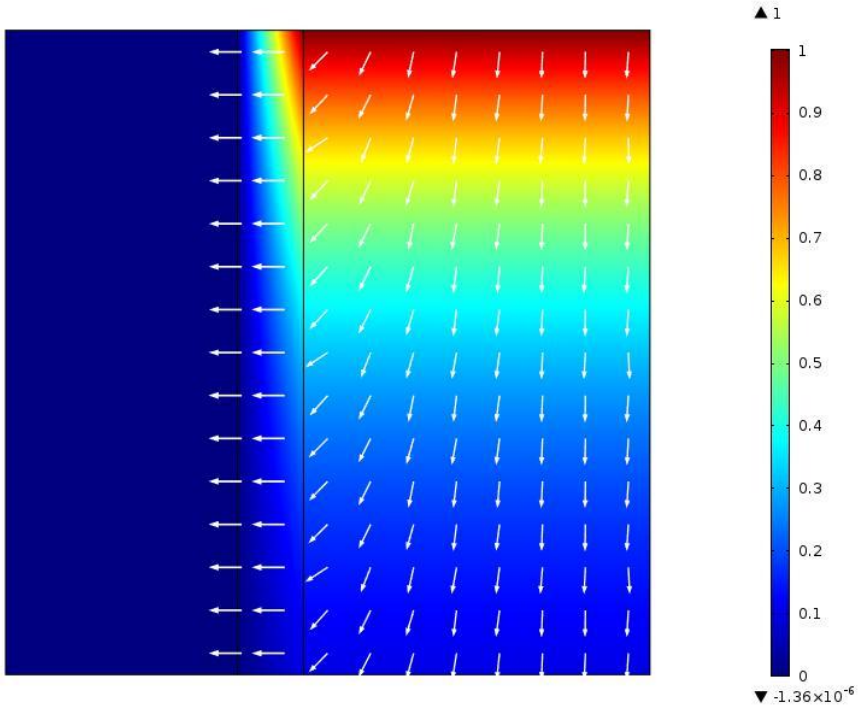

Figure 6
Dimensionless concentration of CO_2; Vl= 0.0503 m/s; Tl= 308 K; Vg= 0.211 m/s; Tg= 298K; PG concentration= 1M.

3.3. Effect of gas and liquid velocity on removal efficiency

In this section, the performance of different absorbents is compared. The effect of liquid (absorbent) velocity on CO_2 capture is presented in Figure 7. As we can see from Figure 7, initially, the removal efficiency of CO_2 is relatively strong and increases as a function of the absorbent velocity. At later stages the removal efficiency of CO_2 weakens, but it still increases as a function of absorbent velocity for MEA, DEA, AMP, PG, and PT absorbents. Therefore, the optimum amount of absorbent could be attained, and costs, due to expensive absorbents and environmental problems assigned to them, will be decreased. It is obvious that as the absorbent velocity increases, the removal efficiency of CO_2 increases because increasing absorbent velocity increases the concentration gradient at the tube-membrane interface; thus, the removal efficiency of CO_2 is increasing. Figure 7 also clearly depicts the fact that PG absorbent has the highest removal efficiency of CO_2, followed by PT, MEA, AMP, DEA, and MDEA in sequence, which is similar to the trend of reaction rate. Amino acids (PG and PT) also have higher partition coefficients which improves the physical absorption and CO_2 capture. It can

be seen from Figure 7 that the removal efficiency of MDEA is much lower than that of the other absorbent, which is ascribed to the reaction rate of MDEA with CO_2.

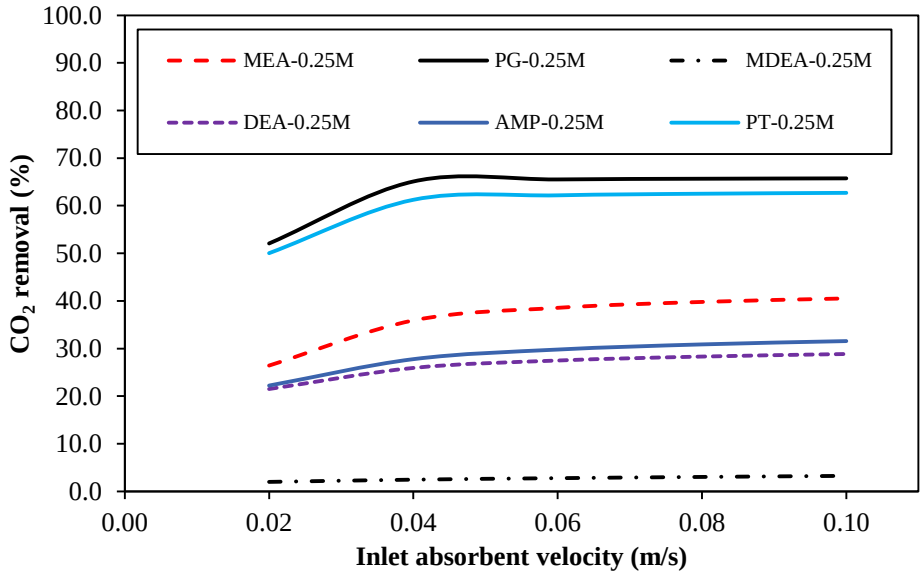

Figure 7
Effect of liquid phase velocity on the removal efficiency of CO_2 for various absorbents; Vg= 0.423 m/s; Tl= 298 K; Tg= 298 K.

Figure 8 illustrates the variation of CO_2 removal efficiency against gas velocity. As expected, increasing gas velocity decreases the residence time of gas phase in the membrane contactor, which leads to decreasing the removal efficiency of CO_2. The trend of removal efficiency of CO_2 for different absorbents is similar to what presented in the previous part.

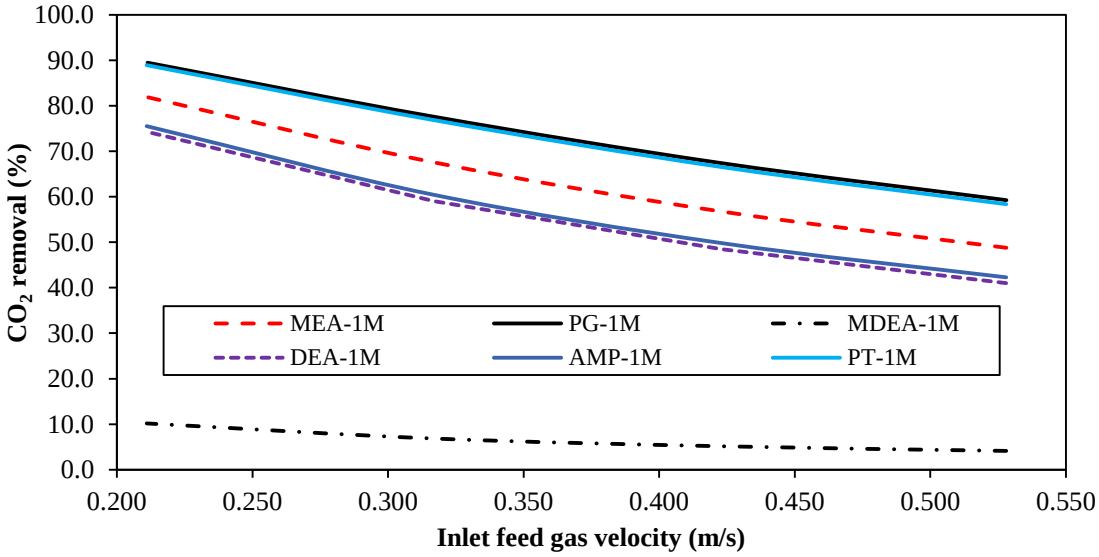

Figure 8
Effect of gas phase velocity on the removal efficiency of CO_2 for various absorbents; Vl= 0.0503 m/s; Tl= 298 K; Tg= 298 K.

Therefore, from the above discussion, it can be concluded that the CO_2 removal efficiency using

different absorbents follows the following sequence: PG> PT> MEA> AMP> DEA> MDEA. Therefore, PG is the preferred absorbent.

3.4. Effect of PG concentration on removal efficiency

Figure 9 illustrates the removal efficiency of CO_2 at various PG inlet temperatures. It is evident that increasing absorbent temperature increases the removal efficiency of CO_2. As the temperature rises, the reaction rate (Kumar et al., 2002; Dindore et al., 2005) and diffusivity (Snijder et al., 1993) of CO_2 in absorbent increase, which results in an increase in the removal efficiency of CO_2. Moreover, increasing absorbent temperature raises the absorbent evaporation (Tan and Chen, 2006), which leads to a reduction in the removal efficiency of CO_2. In this temperature interval (293-313 K), the effect of temperature on the reaction rate and diffusivity is higher than the effect of temperature on evaporating the solvent. At other temperatures, different results may be attained.

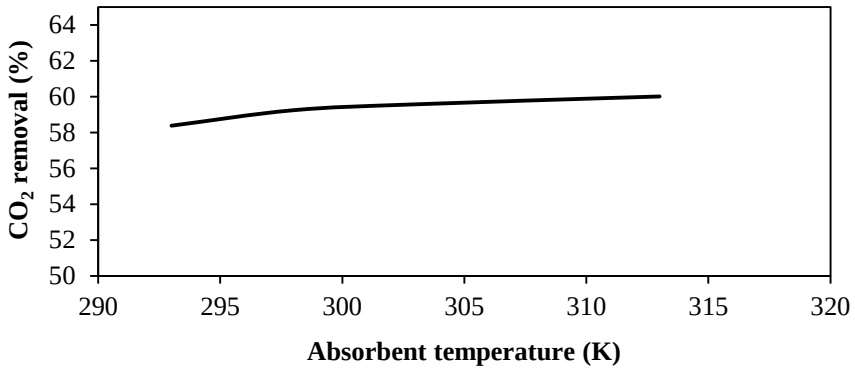

Figure 9
Effect of absorbent temperature on the removal efficiency of CO_2; Vl= 0.0503 m/s; Vg= 0.528 m/s; Tg= 298 K; PG concentration= 1 M.

3.5. Effect of packing density on removal efficiency

The effect of packing density on the removal efficiency of CO_2 is presented in Figure 10. Increasing the number of fibers resulted in an increase in the packing density. In other words, as the packing density increases, the effective area for mass transfer rises, which causes the removal efficiency of CO_2 to improve, even to a hundred percent.

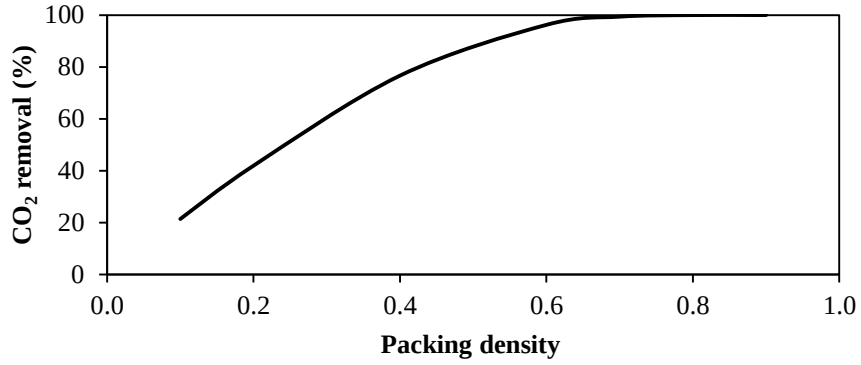

Figure 10
Effect of packing density on the removal efficiency of CO_2; Vl= 0.0503 m/s; Tl= 298 K; Vg= 0.8 m/s; Tg= 298 K; PG concentration= 1M.

3.6. Effect of fiber diameter on removal efficiency

The effect of fiber diameter on the removal efficiency of CO_2 is illustrated in Figure 11. If the inner (R_1) and outer (R_2) radii of fiber are multiplied by enlargement factor (σ), the shell diameter (R_3) is calculated by Equation 12. Therefore, increasing the enlargement factor resulted in an increase in the contact area, which in turn reduces the CO_2 outlet concentration. In agreement with prior expectations, as the enlargement factor increases, the removal efficiency of CO_2 is improved.

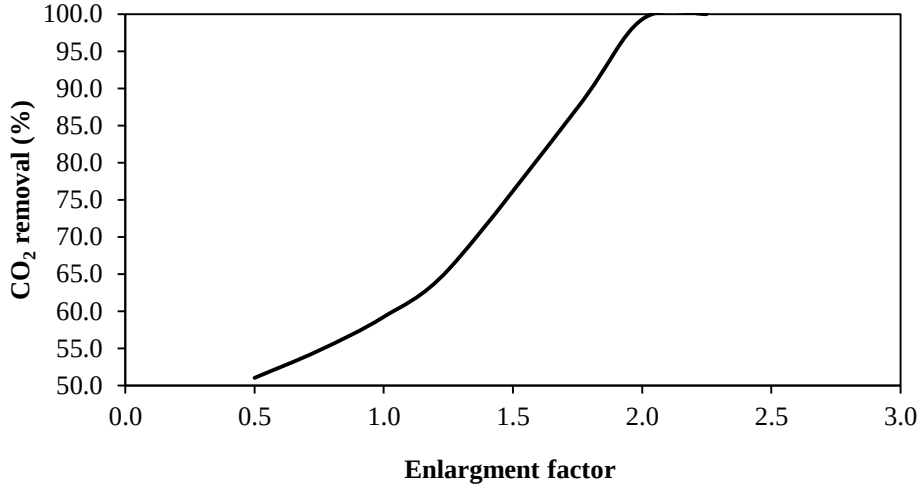

Figure 11
Effect of fiber diameter on the removal efficiency of CO_2; Vl= 0.0503 m/s; Tl= 298 K; Vg= 0.528 m/s; Tg= 298 K; PG concentration= 1 M.

4. Conclusions

A comprehensive two-dimensional mathematical model was developed to describe CO_2 capture by absorption in HFMC using various absorbents. In this study, the performance of six absorbents, namely PG, PT, MEA, AMP, DEA, and MDEA, in removing CO_2 was compared. The model was established for a non-wetted mode and a parallel countercurrent gas-liquid flow arrangement. The radial and axial diffusions in the transport equations were assumed. The equations were solved by FEM, and the model was validated using the results reported by Yan et al. (2007); the simulation results were in good agreement with the experimental data. PG absorbent has the highest removal efficiency of CO_2 followed by PT, MEA, AMP, DEA, and MDEA in sequence. The results of the proposed model indicated that the removal efficiency of CO_2 increased with increasing absorbent velocity, absorbent temperature, packing density, and enlargement factor. Increasing gas velocity in the shell side has a reverse effect on CO_2 removal efficiency. It is worth mentioning that the assumptions of ideal gas may introduce some limitations to the model, and it may not be applicable to high pressures. It is suggested that the effect of using equations of state be investigated in the future works.

Nomenclature

C	: Concentration (M or mol/m^3)
D	: Diffusion coefficient (m^2/s)
L	: Hollow fiber membrane length (cm)

m	: Partition coefficient
n	: Number of hollow fiber
Q	: Volumetric flow rate (m^3/s)
R	: Hollow fiber membrane module radius (cm)
r	: Radial coordinate (m)
R	: Reaction rate ($mol/m^3.s$)
R_1	: Inner radius of fiber (μm)
R_2	: Outer radius of fiber (μm)
Tg	: Inlet gas phase temperature (K)
Tl	: Inlet liquid phase temperature (K)
Vg	: Gas phase velocity (m/s)
Vl	: Liquid phase velocity (m/s)
z	: Axial coordinate (m)
ε	: Membrane porosity
η	: CO_2 removal efficiency
σ	: Enlargement factor
τ	: Membrane tortuosity

References

Al-Marzouqi, M. H., El-Naas, M. H., Marzouk, S. A., Al-Zarooni, M. A., Abdullatif, N., and Faiz, R., Modeling of CO_2 Absorption in Membrane Contactors, Separation and Purification Technology, Vol. 59, No. 3, p. 286-293, 2008.

Al-Marzouqi, M. H., Marzouk, S., El-Naas, A., Abdullatif, M. H., and N., CO_2 Removal from CO_2− CH_4 Gas Mixture Using Different Solvents and Hollow Fiber Membranes, Industrial & Engineering Chemistry Research, Vol. 48, No. 7, p. 3600-3605, 2009.

Atchariyawut, S., Jiraratananon, R., and Wang, R., Separation of CO_2 from CH_4 by Using Gas–liquid Membrane Contacting Process, Journal of Membrane Science, Vol. 304, No. 1, p. 163-172, 2007.

Bird, R. B., Stewart, W. E., and Lightfoot, E. N., Transport Phenomena John Wiley & Sons, New York, p. 413, 1960.

Dindore, V., Brilman, D., and Versteeg, G., Modeling of Cross-flow Membrane Contactors: Mass Transfer with Chemical Reactions, Journal of Membrane Science, Vol. 255, No. 1, p. 275-289, 2005.

Esmaili, J. and Ehsani, M. R., Development of New Potassium Carbonate Sorbent for CO_2 Capture under Real Flue Gas Conditions, Iranian Journal of Oil & Gas Science and Technology, Vol. 3, No. 3, p. 39-46, 2014.

Faiz, R. and Al-Marzouqi, M., Mathematical Modeling for the Simultaneous Absorption of CO_2 and H_2S Using Mea in Hollow Fiber Membrane Contactors, Journal of Membrane Science, Vol. 342, No. 1, p. 269-278, 2009.

Gabelman, A. and S. T. Hwang, Hollow Fiber Membrane Contactors, Journal of Membrane Science, Vol. 159, No. 1, p. 61-106, 1999.

Hamborg, E. S., van Swaaij, W. P., and Versteeg, G. F., Diffusivities in Aqueous Solutions of the Potassium Salt of Amino Acids, Journal of Chemical & Engineering Data, Vol. 53, No. 5, p. 1141-1145, 2008.

Happel, J., Viscous Flow Relative to Arrays of Cylinders, AIChE Journal, Vol. 5, No. 2, p. 174-177, 1959.

Herzog, H., Eliasson, B., and Kaarstad, O., Capturing Greenhouse Gases, Scientific American, Vol. 282, No. 2, p. 72-79, 2000.

Herzog, H. J., What Future for Carbon Capture and Sequestration? Environmental Science & Technology, Vol. 35, No. 7, p. 148A-153A, 2001.

Kumar, P., Hogendoorn J., Feron, P., and Versteeg, G., New Absorption Liquids for the Removal of CO_2 from Dilute Gas Streams Using Membrane Contactors, Chemical Engineering Science, Vol. 57, No. 9, p. 1639-1651, 2002.

Lee, Y., Noble, R. D., Yeom, B. Y., Park, Y. I., and Lee, K. H., Analysis of CO_2 Removal by Hollow Fiber Membrane Contactors, Journal of Membrane Science, Vol. 194, No. 1, p. 57-67, 2001.

Li, J. L. and Chen, B. H., Review of CO_2 Absorption Using Chemical Solvents in Hollow Fiber Membrane Contactors, Separation and Purification Technology, Vol. 41, No. 2, p. 109-122, 2005.

Li, K., Kong, J., and Tan, X., Design of Hollow Fiber Membrane Modules for Soluble Gas Removal, Chemical Engineering Science, Vol. 55, No. 23, p. 5579-5588, 2000.

Liao, C. H. and Li, M. H., Kinetics of Absorption of Carbon Dioxide into Aqueous Solutions of Monoethanolamine+N-Methyldiethanolamine, Chemical Engineering Science, Vol. 57, No. 21, p. 4569-4582, 2002.

Lin, S. H., Chiang, P. C., Hsieh, C.F., Li, M.H., and Tung, K.L., Absorption of Carbon Dioxide by the Absorbent Composed of Piperazine and 2-Amino-2-Methyl-1-Propanol in PVDF Membrane Contactor, Journal of the Chinese Institute of Chemical Engineers, Vol. 39, No. 1, p. 13-21, 2008.

Littel, R., Versteeg, G., and Van Swaaij, W., Kinetics of CO_2 with Primary and Secondary Amines in Aqueous Solutions—II., Influence of Temperature on Zwitterion Formation and Deprotonation Rates, Chemical Engineering Science, Vol. 47, No. 8, p. 2037-2045, 1992.

Lu, J. G., Zheng, Y.F., Cheng, M. D., and Wang, L.J. Effects of Activators on Mass-transfer Enhancement in a Hollow Fiber Contactor Using Activated Alkanolamine Solutions, Journal of Membrane Science, Vol. 289, No. 1, p. 138-149, 2007.

Lyngfelt, A. and Azar, C., Proceedings of Mini-symposium on Carbon Dioxide Capture and Storage, 1999.

Oexmann, J. and Kather, A., Post-combustion CO_2 Capture in Coal-fired Power Plants: Comparison of Integrated Chemical Absorption Processes with Piperazine Promoted Potassium Carbonate and Mea, Energy Procedia, Vol. 1, No. 1, p. 799-806, 2009.

Park, H. H., Deshwal, B. R., Kim, I. W., and Lee, H. K., Absorption of SO_2 from Flue Gas Using PVDF Hollow Fiber Membranes in a Gas–liquid Contactor, Journal of Membrane Science, Vol. 319, No. 1, p. 29-37, 2008.

Paul, S., Ghoshal, A. K., and Mandal, B., Removal of CO_2 by Single and Blended Aqueous Alkanolamine Solvents in Hollow-fiber Membrane Contactor: Modeling and Simulation, Industrial & Engineering Chemistry Research, Vol. 46, No. 8, p. 2576-2588, 2007.

Portugal, A., Derks, P., Versteeg, G., Magalhaes, F., and Mendes, A., Characterization of Potassium Glycinate for Carbon Dioxide Absorption Purposes, Chemical Engineering Science, Vol. 62, No. 23, p. 6534-6547, 2007.

Portugal, A., Magalhaes, F., and Mendes, A., Carbon Dioxide Absorption Kinetics in Potassium Threonate, Chemical Engineering Science, Vol. 63, No. 13, p. 3493-3503, 2008.

Qi, Z. and Cussler, E., Microporous Hollow Fibers for Gas Absorption: II. Mass Transfer across the Membrane, Journal of Membrane Science, Vol. 23, No. 3, p. 333-345, 1985.

Rahmandoost, E., Roozbehani B., and Maddahi, M. H., Experimental Studies of CO_2 Capturing from the Flue Gases, Iranian Journal of Oil & Gas Science and Technology, Vol. 3, No. 4, p. 1-15, 2014.

Ren, J., Wang, R., Zhang, H. Y., Liang, Z. Li, D. T., and Tay, J. H., Effect of PVDF Dope Rheology on the Structure of Hollow Fiber Membranes Used for CO_2 Capture, Journal of Membrane Science, Vol. 281, No. 1, p. 334-344, 2006.

Rezakazemi, M., Niazi, Z., Mirfendereski, M., Shirazian, S., Mohammadi T., and Pak, A., CFD Simulation of Natural Gas Sweetening in a Gas–liquid Hollow-fiber Membrane Contactor, Chemical Engineering Journal, Vol. 168, No. 3, p. 1217-1226, 2011.

Saha, A. K., Bandyopadhyay, S. S., and Biswas, A. K., Solubility and Diffusivity of Nitrous Oxide and Carbon Dioxide in Aqueous Solutions of 2-Amino-2-Methyl-1-Propanol, Journal of Chemical and Engineering Data, Vol. 38, No. 1, p. 78-82, 1993.

Snijder, E. D., Te Riele, M. J., Versteeg, G. F., and Van Swaaij, W., Diffusion Coefficients of Several Aqueous Alkanolamine Solutions, Journal of Chemical and Engineering data, Vol. 38, No. 3, p. 475-480, 1993.

Tan, C. S. and Chen, J. E., Absorption of Carbon Dioxide with Piperazine and its Mixtures in a Rotating Packed Bed, Separation and Purification Technology, Vol. 49, No. 2, p. 174-180, 2006.

Tuinier, M., van Sint Annaland, M., Kramer, G., and Kuipers, J., Cryogenic CO_2 Capture Using Dynamically Operated Packed Beds, Chemical Engineering Science, Vol. 65, No. 1, p. 114-119, 2010.

Versteeg, G. F. and Van Swaalj, W., Solubility and Diffusivity of Acid Gases (Carbon Dioxide, Nitrous Oxide) in Aqueous Alkanolamine Solutions, Journal of Chemical and Engineering Data, Vol. 33, No. 1, p. 29-34, 1988.

Wang, D., Teo, W., and Li, K., Selective Removal of Trace H_2S from Gas Streams Containing CO_2 Using Hollow Fiber Membrane Modules/Contractors, Separation and Purification Technology, Vol. 35, No. 2, p. 125-131, 2004.

Wang, R., Li, D., and Liang, D., Modeling of CO_2 Capture by Three Typical Amine Solutions in Hollow Fiber Membrane Contactors, Chemical Engineering and Processing: Process Intensification, Vol. 43, No. 7, p. 849-856, 2004.

Xu, S., Wang, Y. W., Otto, F. D., and Mather, A. E., Kinetics of the Reaction of Carbon Dioxide with 2-Amino-2-Methyl-1-Propanol Solutions, Chemical Engineering Science, Vol. 51, No. 6, p. 841-850, 1996.

Yan, S. P., Fang, M. X., Zhang, W. F., Wang, S. Y., Xu, Z. K., Luo, Z. Y., and Cen, K. F., Experimental Study on the Separation of CO_2 from Flue Gas Using Hollow Fiber Membrane Contactors without Wetting, Fuel Processing Technology, Vol. 88, No. 5, p. 501-511, 2007.

Zhang, X., Seames, W. S., and Tande, B. M., Recovery of CO_2 from Monoethanolamine Using a Membrane Contactor, Separation Science and Technology, Vol. 49, No. 1, p. 1-11, 2014.

Zhao, L., Riensche, E., Menzer, R., Blum, L., and Stolten, D., A Parametric Study of CO_2/N_2 Gas Separation Membrane Processes for Post-combustion Capture, Journal of Membrane Science, Vol. 325, No. 1, p. 284-294, 2008.